nature medicine

ARTICLES

https://doi.org/10.1038/s41591-021-01557-6

Check for updates

Suppression of mutant *C9orf72* expression by a potent mixed backbone antisense oligonucleotide

Hélène Tran[1,8], Michael P. Moazami[2,8], Huiya Yang[1], Diane McKenna-Yasek[1], Catherine L. Douthwright[1], Courtney Pinto[1], Jake Metterville[1], Minwook Shin[2], Nitasha Sanil[3], Craig Dooley[3], Ajit Puri[4], Alexandra Weiss[1], Nicholas Wightman[1], Heather Gray-Edwards[4], Miklos Marosfoi[4], Robert M. King[4,5], Thomas Kenderdine[6], Daniele Fabris[6], Robert Bowser[7], Jonathan K. Watts[2] ✉ and Robert H. Brown Jr[1] ✉

Expansions of a G_4C_2 repeat in the *C9ORF72* gene are the most common genetic cause of amyotrophic lateral sclerosis (ALS) and frontotemporal dementia (FTD), two devastating adult-onset neurodegenerative disorders. Using C9-ALS/FTD patient-derived cells and *C9ORF72* BAC transgenic mice, we generated and optimized antisense oligonucleotides (ASOs) that selectively blunt expression of G_4C_2 repeat-containing transcripts and effectively suppress tissue levels of poly(GP) dipeptides. ASOs with reduced phosphorothioate content showed improved tolerability without sacrificing efficacy. In a single patient harboring mutant *C9ORF72* with the G_4C_2 repeat expansion, repeated dosing by intrathecal delivery of the optimal ASO was well tolerated, leading to significant reductions in levels of cerebrospinal fluid poly(GP). This report provides insight into the effect of nucleic acid chemistry on toxicity and, to our knowledge, for the first time demonstrates the feasibility of clinical suppression of the *C9ORF72* gene. Additional clinical trials will be required to demonstrate safety and efficacy of this therapy in patients with *C9ORF72* gene mutations.

A GGGGCC (G_4C_2) hexanucleotide repeat expansion (HRE) in the first intron of the *C9ORF72* (C9) gene is the most common genetic cause of ALS and FTD, two devastating adult-onset neurodegenerative disorders[1,2]. Proposed disease mechanisms include a partial loss of the C9ORF72 protein function (C9ORF72 haploinsufficiency) and acquired toxicity of the repeat expansion[3]. Transcription of the *C9ORF72* gene generates three transcript variants: V1, V2 and V3 (Fig. 1a). V1 is translated to produce a short protein isoform (222 amino acids), whereas V2 and V3 generate the most predominant C9ORF72 protein (481 amino acids), which functions in vesicular trafficking[4]. Located adjacent to the promoter region of the most abundant V2 transcript variant, the G_4C_2 repeat expansion impairs its transcription, leading to C9ORF72 protein haploinsufficiency[5,6], impaired function of myeloid cells[7,8] and diminished neuronal viability[9]. Both sense and antisense transcripts encompassing the HRE in V1 and V3 generate RNA foci and undergo translation into atypical, aggregation-prone dipeptide repeat (DPR) proteins in all open reading frames[10,11]. These unusual DPRs are toxic in several experimental model systems[12–15]. Despite important advances in elucidating the molecular pathology of the expanded hexanucleotide repeats, there are no meaningful therapies for *C9ORF72*-related ALS or FTD.

ASOs can drive therapeutic effects by mechanisms that include splice-modulation or, if the ASO contains DNA, activation of endogenous RNase H[16] to degrade the target RNA. The broad bioavailability of ASOs in the central nervous system (CNS), including both neurons and glial cells[17], has prompted development of ASOs as therapy for dominantly transmitted genetic disorders of the CNS (for example, ALS caused by mutations in the SOD1 gene).

Here we report development of ASOs targeting *C9ORF72* to treat ALS and FTD. Using different C9-related model systems, including patient-derived samples and two C9BAC transgenic mouse models[18,19], we generated ASOs that specifically reduce levels of the transcripts harboring the HRE as well as their DPR products, with minimal effects on the most abundant V2 isoform, which does not contain the HRE. We show that modification of a subset of the phosphodiester internucleoside linkages significantly improves ASO tolerability without impairing potency. We demonstrate that, in a single patient harboring mutant *C9ORF72* with the G_4C_2 repeat expressions, repeated intrathecal dosing of the optimal ASO was well tolerated and led to significant and durable reduction in levels of cerebrospinal fluid (CSF) poly(GP).

Results

ASO suppresses *C9ORF72* in fibroblasts and mouse neurons. Because haploinsufficiency of *C9ORF72* is thought to be adverse, we developed ASOs that target only the 5′ end of transcripts V1 and V3 that bear the G_4C_2 repeat expansion, sparing transcript V2. As it is not fully clear whether the repeat-containing intron is retained or spliced out, we focused our effort on ASO sequences targeting the intron repeat junction (Fig. 1a). Others previously tested ASOs against this target region in patient-derived samples with success

[1]Department of Neurology, University of Massachusetts Medical School, Worcester, MA, USA. [2]RNA Therapeutics Institute, University of Massachusetts Medical School, Worcester, MA, USA. [3]Research Pharmacy, University of Massachusetts Medical School, Worcester, MA, USA. [4]Department of Radiology, University of Massachusetts Medical School, Worcester, MA, USA. [5]Department of Biomedical Engineering, Worcester Polytechnic Institute, Worcester, MA, USA. [6]Department of Chemistry, University of Connecticut, Storrs, CT, USA. [7]Departments of Neurology and Neurobiology, Barrow Neurological Institute, Phoenix, AZ, USA. [8]These authors contributed equally: Hélène Tran, Michael P. Moazami. ✉e-mail: jonathan.watts@umassmed.edu; robert.brown@umassmed.edu

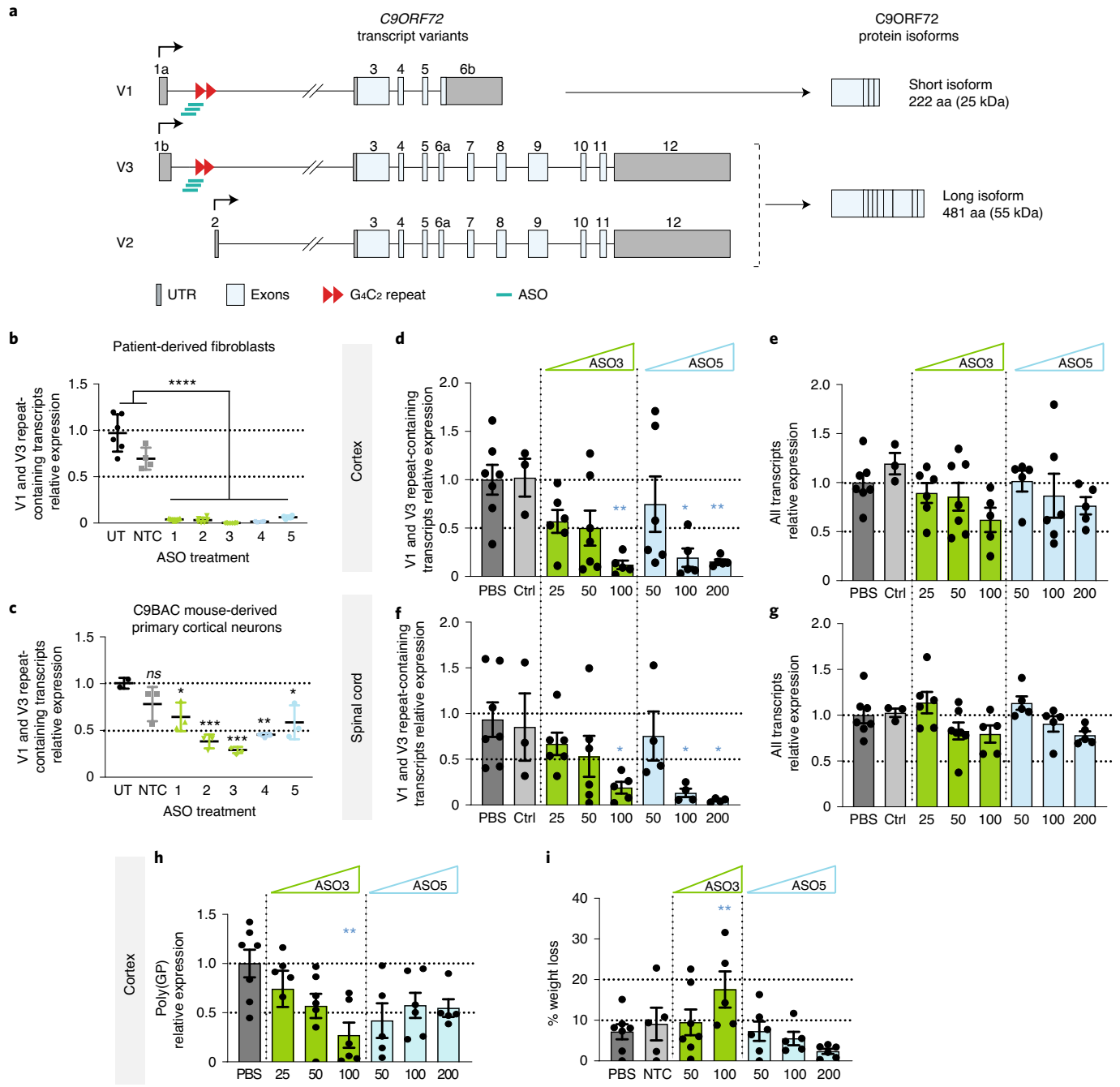

Fig. 1 | G_4C_2-targeting LNA- and MOE-modified ASOs reduce the *C9ORF72* repeat-containing transcripts in patient-derived fibroblasts, C9BAC mouse-derived neurons and C9BAC mice. a, Schematic of *C9ORF72* transcript variants and of the two protein isoforms as named in PubMed. The repeat expansion (red triangles) located in the first intron is expressed in V1 and V3. V2, the most abundant, starts from a different transcription start site (black arrow) and does not include the repeat expansion. V2 and V3 encode the main C9ORF72 protein isoform. Gray boxes represent untranslated regions (UTR); light blue boxes represent exons; and black lines represent introns. ASOs used in this study (green bars) target the intronic region flanking the repeat expansion. **b**, LNA and 2′-O-MOE ASOs dramatically reduce the level of repeat-containing transcripts at a dose of 100 nM 72 h after lipid-mediated delivery in patient-derived fibroblasts as measured by qRT–PCR. $n = 6$; each data point is derived from a separate well. $^{****}P < 0.0001$, comparing any treatment group to either control group, based on one-way ANOVA with Dunnett's multiple comparisons test. **c**, LNA and 2′-O-MOE ASOs significantly reduce the level of repeat-containing transcripts after 2 weeks of treatment with 1 μM ASO without lipid assistance (gymnotic delivery) in primary cortical neurons derived from C9BAC mice. $n = 3$; each data point is derived from a separate well. NS, not significant ($P = 0.23$), comparing the non-targeting control (NTC) group to the PBS group, based on one-way ANOVA with Dunnett's multiple comparisons test. **d–g**, Expression of V1–V3 repeat-containing transcripts (**d**, **f**) and all transcripts (**e**, **g**) in cortex and spinal cord quantified by qRT–PCR in mice infused with PBS (dark gray), NTC ASO (light gray), ASO3 (green) or ASO5 (blue) at the indicated dose. For each dose level, $n = 5$–7, except the NTC group ($n = 3$). **h**, Relative expression of poly(GP) in the cortex of mice treated with ASO3 (green) and ASO5 (blue) assayed by sandwich immunoassay. Data are represented as mean ± s.e.m. **i**, percent of body weight loss at end point relative to before treatment. In all panels, $^{*}P < 0.05$, $^{**}P < 0.01$ and $^{***}P < 0.001$, comparing treatment groups to the PBS group, based on one-way ANOVA with Dunnett's multiple comparisons test. All replicates are shown as individual data points. In **d–i**, each data point is derived from a separate animal. aa, amino acid; Ctrl, control; UT, untreated.

Table 1 | ASO sequences and modification patterns

Name	Sequences and modification pattern[a]
ASO1	***CCC***TAGCGCGCG***ACT***
ASO2	***CC***CGGCCCCTAGCGCGCG***AC***
ASO3	***GC***CCCTAGCGCGCGAC***TC***
ASO4	**CCCGG**CCCCTAGCGC**GCGAC**
ASO5	**GCCCC**TAGCGCGC**GACTC**
ASO5-1	**GCoCoCoCo**TAGCGCGC**oGoAoCoTC**
ASO5-2	**GCoCoCoC**TAGCGCGC**GoAoCoTC**

[a]Normal text, DNA; bold italic text, LNA; bold underlined text, MOE. All C residues are 5-methyl cytidine. All linkages are PS except where PO linkages are indicated by 'o'.

both in vitro[20,21] and in vivo in mice[22–25] and flies[26]. We designed locked nucleic acid (LNA) and 2′-O-methoxyethyl (MOE) gapmer ASOs (Table 1). All cytosine residues were 5-methylated to reduce immunogenicity.

We tested ASOs in multiple steps. We first developed a dual-luciferase screen for ASOs that suppress expression of transcripts V1, V2 and V3 (Supplementary Fig. 1a) and used this assay to narrow our focus to five ASOs. We then treated primary C9-ALS/FTD patient-derived fibroblasts (containing >1,000 repeats, Supplementary Fig. 1b, and showing visible nuclear *C9ORF72* foci, Supplementary Fig. 1c) with ASOs 1–5 at a dose of 100 nM by lipid transfection. After 72 h, all five ASOs reduced V1–V3 expression to almost undetectable levels (Fig. 1b). Silencing was dose dependent in patient-derived fibroblasts (Supplementary Fig. 1d) and in HEK293 cells expressing the dual-luciferase reporter (Supplementary Fig. 1e).

A hallmark of C9-ALS/FTD is the presence of repeat-containing RNA foci[1,2,20,21,27,28]. Three days after ASO treatment, the number of cells with foci was reduced from 80% (untreated) to 20–40% (treated). Moreover, fewer foci per cell were detected, showing that all five ASOs were potent inhibitors of G_4C_2 RNA foci (Supplementary Fig. 1f,g).

Each of the five ASOs was also active by lipid-free delivery to neurons. Primary cortical neurons were derived from E15.5 C9BAC embryos and treated with 1 μM ASO at 5 days in vitro. Fifteen days after treatment, expression of human repeat-containing transcript was significantly reduced in all treated conditions compared to the non-targeting control or untreated condition (Fig. 1c).

ASOs suppress *C9ORF72* in C9BAC neurons. We next evaluated the properties of these ASOs in vivo in wild-type (WT) and *C9ORF72* transgenic mice. ASOs can be delivered to the brain tissue and spinal cord through the surrounding CSF via an intracerebroventricular (ICV) bolus injection or osmotic pump infusion[29]. ASO3 and ASO5 distributed broadly throughout the mouse CNS and showed neuronal uptake (Supplementary Fig. 2).

We first assessed ASO tolerability in WT C57BL/6 mice. Each animal received a single ICV bolus dose of one of our five ASOs (Table 1). Mice injected with ASOs 1, 2 and 4 had severe seizure-like phenotypes upon recovery from anesthesia or did not survive 24 h after injection, whereas mice treated with ASOs 3 and 5 recovered well after injection.

We then compared the tolerability and efficacy of ASOs 3 and 5 in C9BAC transgenic mice. C9BAC transgenic mice generated in our laboratory expressed approximately 600 G_4C_2 repeat motifs within a truncated human *C9ORF72* gene (from exons 1–6). Although these mice do not develop a motor phenotype, they recapitulate disease hallmarks, including repeat-containing RNA foci and dipeptide repeat (DPR)[18]. In our C9BAC mice, we were not able to safely perform ICV bolus injections with more than 10 nmol of LNA-modified ASO3 due to induction of severe motor phenotypes. To overcome this limitation, we used osmotic pumps to compare the potency of ASO3 and ASO5. Doses ranging from 2.5 to 20 nmol per day of each ASO were continuously infused over 10 d into the right lateral ventricle of age-matched heterozygous C9BAC mice through a cannula using an implanted Alzet osmotic pump. The cortex and spinal regions of animals treated with ASO3 and ASO5 demonstrated potent, dose-dependent reduction in V1 and V3 repeat-containing transcripts in both the cortex and spinal cord regions (Fig. 1d,f). Notably, despite their effect on V1 and V3, neither ASO3 nor ASO5 produced any substantial reduction of the level of the V2 transcript (and, hence, the total *C9ORF72* transcript variants) (Fig. 1e, g). Poly(GP) DPR was also reduced in the cortex of mice treated with both ASO3 and ASO5 (Fig. 1h).

Neither ASO produced adverse behavioral side effects; all animals remained healthy until they were sacrificed at 21 d. Routine clinical blood chemistry and liver and kidney morphology after hematoxylin and eosin (H&E) staining revealed no gross abnormalities. At the 100-nmol dose, mice receiving ASO3 showed more weight loss than mice in the other groups (18%) (Fig. 1i). We, therefore, focused on ASO5 for further optimization.

Phosphorothioate reduction optimizes ASO5 safety and activity in mice. Bolus injections of 50 nmol or higher induced severe motor phenotypes in the first hours after injection. This low maximum tolerated dose (MTD) notably limits the dosing scheme and narrows the therapeutic window. We, therefore, sought to improve the efficacy and tolerability of ASO5.

ASO5 has a fully modified phosphorothioate (PS) backbone. The PS modification confers nuclease stability and increased protein binding, which leads to increased cellular uptake but can also lead to toxicity[30]. We sought to reduce the number of PS linkages to generate a less toxic ASO without compromising activity[31–33]. We reduced the PS content within the 5′ and 3′ MOE-modified 'wings' of the ASO, maintaining PS modification throughout the DNA gap. ASO5-1 and ASO5-2 differed only in the presence or absence of a PS linkage between nucleotides 5–6 and 13–14 (Table 1). Both of these analogues showed reduced motor phenotypes and a higher MTD than ASO5. Elsewhere, we explore the mechanism of the motor phenotypes observed here and follow-up on the improvement observed by mixed backbone modification patterns[34].

We administered 30 nmol of each ASO via a bolus ICV injection in C9BAC mice and analyzed efficacy at 8 weeks (Fig. 2a–f). Mice treated with 30 nmol of ASO5 and ASO5-2 had a significantly reduced level of V1 and V3 transcripts in cortex and spinal cord compared to the PBS-treated group (Fig. 2a,d) with minimal effect on total transcripts (Fig. 2b,e), showing that absence of PS inter-nucleotide linkages between two MOE-modified nucleotides did not impair biological activity in vivo. By contrast, ASO5-1, which lacked the PS linkage at the junction between the MOE wings and the DNA gap, achieved only ~ 25% knockdown of V1–V3 at a 30-nmol dose (Fig. 2a,d). Dose–response studies confirmed the superior efficacy and potency of ASO5 and ASO5-2 relative to ASO5-1 (Supplementary Fig. 3). ASO5-2 treatment also reduced poly(GP) levels in cortex and spinal cord (Fig. 2c,f). Based on its efficacy and tolerability profile, we selected ASO5-2 as our lead compound.

Sustained potency of mixed backbone ASO5-2 in two mouse models. We next tested the in vivo dose dependence of ASO5-2, which revealed an ED_{50} of 4.75 nmol (Fig. 2g) for V1–V3 RNA silencing in the cortex of C9BAC mice 3 weeks after treatment. At the same time point, ASO5-2 also significantly and dose dependently reduced levels of poly(GP) in a dose-dependent manner (Fig. 2h).

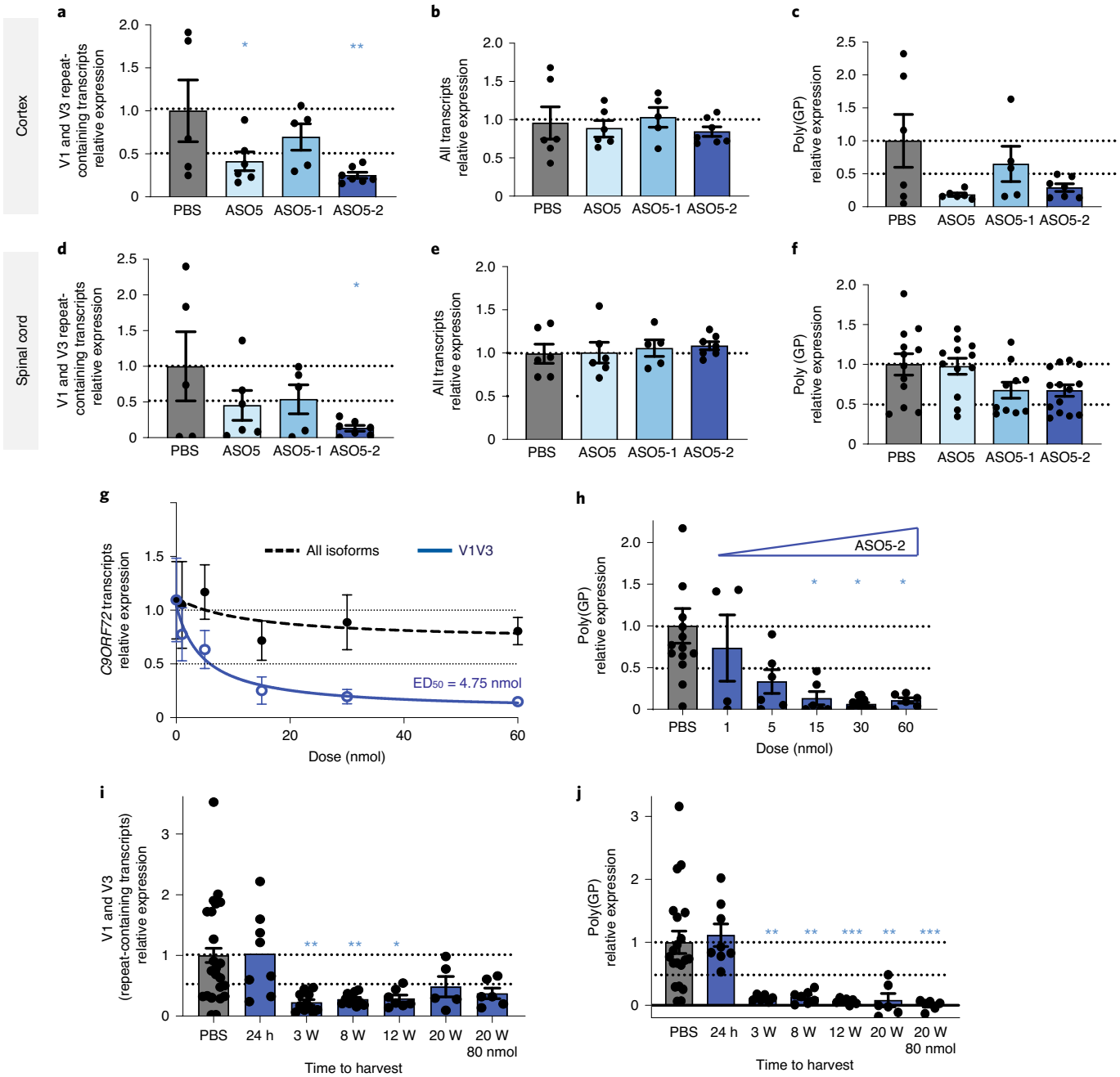

Fig. 2 | Analogues of ASO5 with reduced PS content maintain robust and durable biological activity after CNS administration in heterozygous C9BAC mice. a–f, A single-dose infusion shows robust silencing of V1–V3 repeat-containing transcripts (**a**, **d**) with minimal change in overall *C9ORF72* RNA levels (**b**, **e**) in cortex and spinal cord quantified by qRT-PCR, along with a robust drop in levels of poly(GP) (**c**, **f**) in mice treated with PBS (dark gray), ASO5 (light blue), ASO5-1 (medium blue) and ASO5-2 (dark blue) 8 weeks after administration of 30 nmol of each ASO. For each ASO group, $n = 5$–7. **g**, **h**, Dose-dependent silencing of *C9ORF72* transcripts (**g**) and poly(GP) (**h**) after a single injection of 1, 5, 15, 30 or 60 nmol of ASO5-2 relative to PBS control. ASO 5-2 was administered into the lateral ventricle of 5–6-month-old heterozygous C9BAC mice, and expression of RNA and dipeptide levels was evaluated after 3 weeks. For each ASO group, $n = 5$–7. **i**, **j**, A time course experiment was performed in heterozygous C9BAC mice treated with 30 nmol of ASO5-2: tissues were collected and analyzed at 24 h or 3, 8, 12 and 20 weeks after treatment; an 80-nmol dose was also harvested at 20 weeks only. Expression of V1 and V3 repeat-containing transcripts (**i**) and poly(GP) (**j**) was analyzed in cortex 24 h or 3, 8, 12 or 20 weeks after a single-dose injection of ASO5-2. In all panels, $^{*}P < 0.05$, $^{**}P < 0.01$ and $^{***}P < 0.001$, comparing treatment groups to the PBS group, based on one-way ANOVA with Dunnett's multiple comparisons test. In **a**–**f** and **h**–**j**, each data point is derived from a separate animal. W, weeks.

We also evaluated the duration of effect of ASO5-2. Our initial studies showed that absence of PS linkages flanked by MOE nucleotides (as in ASO5-2) did not impair biological activity in vitro and in vivo 3 weeks after treatment. However, because PS linkages also protect ASOs from nuclease degradation, we wondered if the duration of effect of ASO5-2 would be similar to its fully PS-modified parent ASO5. To address this question, we injected C9BAC transgenic mice with 30 nmol of ASO5-2 and analyzed the level of V1–

Table 2 | CSF parameters in relation to dosing of ASO5-1 in a patient

	Chems[1]			ASO	ASO	GP			Tube 1		Tube n			Differential Tube 1				Differential Tube n			
Date	Weeks	Glu	Pro	Dose[2]	Level[3]	Rel[4]	pNFH[5]	NFL[6]	WBC[7]	RBC[8]	WBC	RBC	*n*	Cells	Lymphs	Monos	Polys	Cells	Lymphs	Monos	Polys
05/9/16		71	56		0	1.00			2	37	1	5	3	16	31	63	6	100	45	54	1
8/24/19	0		59	0.5	0	1.00	253.8	2,249.8			0	0	4	5	100						
9/9/19	2	65	48	1.0	11.7	1.05	309.2	2,478.2			1	2	4	50	36	64					
10/7/19	6	62	52		19.9	1.08	444.8	2,840.3			1	0	4	18	67	33					
1/16/20	20.4	69	54	1.5	1.7	0.62	353.4	2,922.0	1	3	2	0	4	9	67	33		4	50	50	
1/30/20	22.4	71	54		20.5	0.62	299.4	3,212.4	3	211	1	2	4	100	58	36	6	36	67	33	
2/13/20	24.4	59	55	2.0	15.1	0.53	350.2	3,078.4	1	3	1	1	3	27	74	26		11	55	45	
2/26/20	26.3	65	65		42.5	0.37	516.7	3,687.9	1	1	1	1	3	42	45	55		50	44	56	
3/9/20	28.0	64	52	2.0	26.1	0.38	442.4	4,137.3	3	1	1	1	3	66	58	42		81	62	38	
4/23/20	34.4	67	62		17.7	0.24	810.8	11,269.3	4	173	8	1	3	100	41	58	1	100	54	46	
5/4/20	36.0	65	66	2.0	14.4	0.21	1,156.3	13,626.6	11	0	3	2	3	100	58	42	6	6	67	33	
7/27/20	48.0	67	49	2.0	9.33	0.23	1,337.9	2,790.5	8	4	3	7	2	23	78	22		100	65	33	2
10/20/20	60.1	66	40	2.0	8.9	0.30	966.2	10,361.5	2	1	1	0	3	19	47	33		58	62	48	3

[1] mg dl^{-1}; [2] ng ml^{-1} (baseline, 0.01–0.03 ng ml^{-1}); [3] cells per ml [4] mg dl^{-1}; [5] pg/ml^{-1} (normal, 2–300; ALS, 250–12,000); [6] cells per ml [7] ng ml^{-1}; [8] pg ml^{-1} (normal, 100–1,500; ALS, 1,000–20,000) Cells, number per ml; GP Rel, poly(GP) level relative to baseline; Glu, glucose; Lymphs, lymphocytes; Monos, monocytes; Polys, polymorphonuclear cells; Pro, protein; RBC, red blood cell count; WBC, white blood cell count.

V3 transcripts 24 h or 3, 8 or 20 weeks after injection (Fig. 2i). No effect was observed on the V1–V3 target RNA 24 h after injection. However, a significant, specific, dose-dependent reduction of ~80% of V1–V3 transcripts, but not total C9 transcripts, was observed 3 weeks after injection, and, notably, this was sustained up to 20 weeks in the cortex (Fig. 2i). Analogously, we also observed a sustained reduction in the levels of the poly(GP) proteins, approaching 90% reduction even at 20 weeks after the single injection of 30-nmol ASO5-2 (Fig. 2j).

No significant body weight loss or behavioral adverse events (as defined in the Methods) were detected in animals treated with ASO5-2 or the PBS control (Supplementary Fig. 4a). Likewise, no change in liver or spleen weight or morphology was observed (Supplementary Fig. 4b–d). Finally, to further assay the tolerability of ASO5-2 treatment, we analyzed the coordinated motor functions of mice treated with ASO5-2 or injected with vehicle PBS. Seven mice per group were tested in a blinded manner on their rotarod performance weekly after treatment for 19 weeks. No motor deficit was observed in the treated group, underlining the tolerability of ASO treatment (Supplementary Fig. 4e).

From these observations, we concluded that ASO5-2 can be safely administered to transgenic C9BAC mice via ICV delivery and that this durably suppresses the offending V1 and V3 transcripts, but not the V2 transcript, of *C9ORF72* as well as the toxic poly(GP) dipeptides.

ASO5-2 is non-toxic in large animals. Encouraged by safety and efficacy data in the C9BAC mice, we next obtained additional preclinical toxicity profiles in large animals, focusing on ASO5-2 as our lead ASO. As a pilot behavioral study, we performed an intrathecal injection of ASO5-2 at 2 mg kg^{-1} in four sheep. For intrathecal injection in sheep, it was necessary to thread a microcatheter up though the intrathecal space and deliver the ASO directly into the cisterna magna (Methods)[34]. Intracisternal contrast injection and cone beam computed tomography confirmed the correct catheter position before ASO injection. At 1 month, the sheep showed no neurological abnormalities.

We then purchased a batch of Good Manufacturing Practices (GMP)-grade ASO5-2 (ChemGenes). The sequence and modification pattern of the GMP ASO was confirmed by mass spectrometry fragment analysis (Supplementary Fig. 5).

We engaged an outside laboratory (Charles River Laboratories) to conduct a Good Laboratory Practices safety study of ASO5-2 in cynomolgus monkeys. Twenty-eight normal monkeys averaging 2.5 kg in weight were treated with 0 ($n=8$), 1.5 ($n=12$) or 6.0 ($n=8$) mg of ASO5-2. Necropsy was performed at 29 d or 90 d (half the animals at each time point). Treatment was by intrathecal injection on days 1, 14 and 28 for animals assigned to the day 29 and day 90 necropsies and additionally on days 57 and 85 for animals assigned to the day 90 necropsy. No behavioral or neurological deficits were observed out to 90 d at either dose; the necropsies did not show pathological findings attributable to ASO5-2 (data not shown).

ASO5-2 suppresses poly(GP) levels in a *C9ORF72* patient. Further encouraged by the large animal studies, we administered ASO5-2, which we have designated afinersen, in ascending doses to a single individual patient with atypical motor neuron dysfunction who harbored a *C9ORF72* mutation, with appropriate authorization by the Western Institutional Review Board and the US Food and Drug Administration (FDA) (IND141673). This individual was a 60-year-old male with a *C9ORF72* G_4C_2 expansion of approximately 2,400 repeats. He was assessed neurologically because of recurrent left foot drop induced by distance running, followed by slowly progressive weakness in the feet and hands. On examination, he showed distal weakness in the legs and diffuse hyporeflexia and

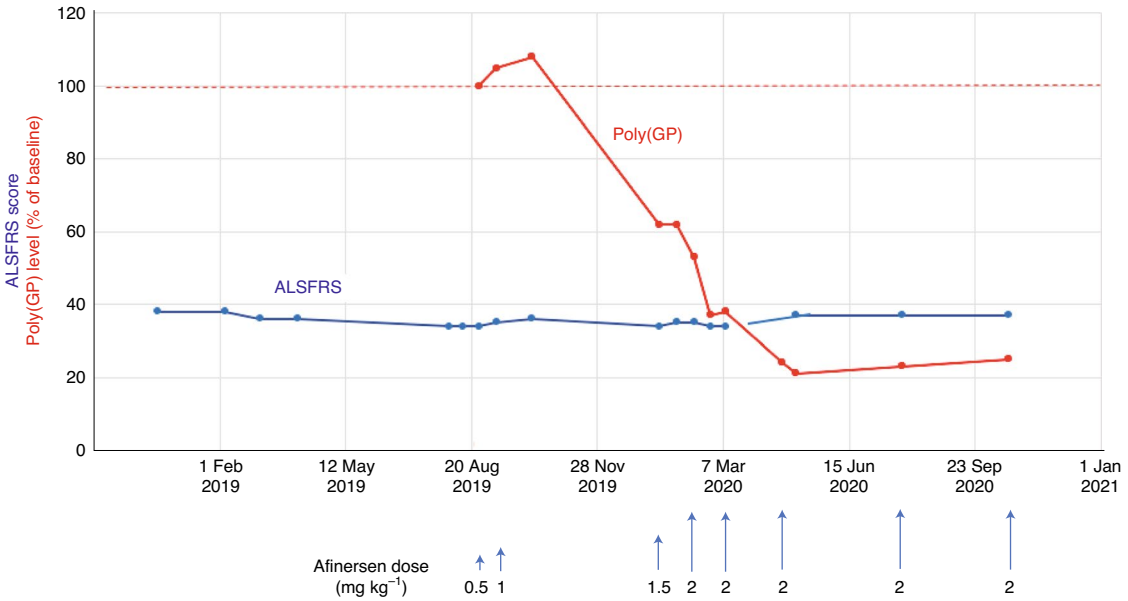

Fig. 3 | Clinical summary and afinersen (ASO5-2) dosing. A single patient received multiple doses of ASO5-2 as indicated with arrows below the graph. The patient's ALSFRS score before and during treatment is shown as a blue line and points. The patient's poly(GP) DPR level, relative to the baseline (100%), is shown as a red line and points.

subtle sensory loss in the distal legs and feet. Physiological studies documented focally enlarged motor units with evidence of scattered foci of active denervation. CSF analysis revealed elevated levels of poly(GP) DPSs (Table 2) but was otherwise benign. As summarized in Fig. 3, on 29 August 2019, the patient was treated with intrathecal ASO5-2 at 0.5 mg kg^{-1}, followed by 1.0 mg kg^{-1} 2 weeks later. On 26 January 2020, he received a third dose at 1.5 mg kg^{-1}, increased to 2.0 mg kg^{-1} on 13 February; 2.0 mg kg^{-1} was subsequently administered four more times (Fig. 3). He experienced no medically or neurologically adverse effects from these interventions, and his laboratory safety studies were unremarkable. In multiple CSF evaluations (Table 2), his CSF cell counts and protein and glucose levels were largely unremarkable. At the time of the fourth and fifth CSF analyses, he showed very mild pleocytosis (but not in both CSF tubes on a given day). He also showed a progressive increase in CSF phosphorylated neurofilament heavy and neurofilament light chains (Table 2), which peaked after the fourth 2.0 mg kg^{-1} dose of ASO5-2 and then partially subsided as the interval between doses was extended.

The toxic polydipeptides translated from the expanded hexanucleotide repeat are detectable in the CSF of patients with ALS. We monitored poly(GP) levels as a biomarker to ascertain the efficacy of silencing of the repeat-containing transcripts. The patient's CSF poly(GP) levels in two samples before dosing were in the range 0.01–0.03 ng ml^{-1}. After sequential doses of 2.0 mg kg^{-1}, the relative CSF poly(GP) levels dropped by approximately 80%, correlating with increasing CNS levels of ASO5-2 (Fig. 3 and Table 2). During the months of treatment, the patient's Amyotrophic Lateral Sclerosis Functional Rating Scale (ALSFRS) score was largely stable. Initially, it was 38 (48 is normal), decreasing to a nadir of 33, but then improving to 38 concomitantly with the higher doses of ASO5-2.

We also monitored levels of ASO5-2 within the patient's CSF (Supplementary Fig. 6). The data showed an excellent fit to a two-phase exponential curve, reflecting a fast phase presumably due to initial clearance from CSF ($t_{1/2}$ 4.7 d), followed by slow clearance ($t_{1/2}$ 4.8 weeks). A dose of 2 mg kg^{-1} every 3 months showed stable levels of ASO in CSF and stable silencing of poly(GP).

Discussion

Ten years after the identification of the G_4C_2 repeat expansion in the gene *C9ORF72* as the most common genetic cause of ALS and FTD, multiple investigations have defined potential disease mechanisms. Partial loss of function of *C9ORF72* likely contributes to the neurotoxicity of hexanucleotide expansions but does not, by itself, recapitulate motor neuron degeneration[5,35]. Forced expression of mutant human *C9ORF72* in mice also fails to reproduce frank motor neuron pathology but does replicate important molecular signatures, including intranuclear RNA foci and cytoplasmic polydipeptides. These are generated selectively by two of the three *C9ORF72* transcripts, V1 and V3, that harbor hexanucleotide expansions. Together, these observations suggest that an effective therapeutic strategy will be to suppress expression of V1 and V3 to reduce levels of repeat-containing RNA and polydipeptides while maintaining baseline levels of V2, which produces the full-length C9ORF72 protein and, thereby, avoids haploinsufficiency. Here we report that ASOs targeting the 5′ junction of the expanded repeat selectively reduce *C9ORF72* repeat-containing transcripts V1 and V3 in a dose-dependent manner after ICV administration in C9BAC transgenic mice, without reducing the overall level of *C9ORF72* V2 transcripts. This intervention significantly reduces numbers of intranuclear RNA foci and depresses the level of poly(GP) dipeptides, which are predicted to be produced from both sense and anti-sense strands of the hexanucleotide repeat. Moreover, in a single patient, this also reduced poly(GP) dipeptide levels by approximately 80%.

This report confirms earlier reports that ASOs can suppress V1 and V3 transcripts in C9-ALS/FTD[20–26] and extends understanding of this therapeutic approach in several important ways. Notably, we examined the effect of modifications of the backbone on both the potency and toxicity of the ASOs. Reducing the degree of PS modification substantially increased the acute tolerability in the CNS without impairing its potent biological activity. Although there are published examples of mixed backbone ASOs used in the CNS[31–33,36–39], to our knowledge this is the first presentation of comparative data on the efficacy and tolerability of fully versus partially PS-modified ASOs and the first to highlight the critical importance

of the position of PS modifications in maintaining efficacy while reducing toxicity.

In the course of these studies of ribose and backbone modifications, we compared the efficacy of ICV bolus versus chronically administered ASOs. It appears that, for similar doses, delivery by bolus is more effective than by pump. For example, V1–V3 transcripts were reduced ~80% by ASO5 at 30 nmol delivered by intraveneous bolus, whereas pump delivery of 50 nmol failed to reduce levels of these transcripts. An analogous difference was observed in ASO therapy in a murine model of spinal muscular atrophy[29], in which bolus administration proved more effective than chronic infusion.

The observed efficacy in mice and safety in both mice and primates prompted our study of repeated dosing of ASO5-2 via intrathecal delivery in a single patient. This was well tolerated as gauged by clinical examination and the safety profile in blood and CSF (Table 2). With repeated dosing of ASO5-2, we observed a progressive but transient elevation of two CSF biomarkers: phosphorylated neurofilament and neurofilament light chains. We ascribe this to some degree of nerve root irritation provoked by the intrathecal ASO or to some component of the disease not influenced by ASO5-2. This phenomenon is described in the literature in humans but, fortunately, has not been associated with major neurological consequences[40]. In our case, these biomarkers subsided somewhat in the later CSFs, as the interval between dosing was extended, suggesting a dose–response relation. The patient's clinical metrics improved across the course of therapy, despite the increment in the CSF neurofilament biomarkers.

Most notably, our study provides proof of concept that ASO therapy in a human can effectively and safely suppress levels of the *C9ORF72* transcript that harbor expansions (V1 and V3) without significantly affecting the predominant V2 transcript. In our models in vitro and in vivo, and in an individual with a *C9ORF72* expansion, we observed an 80% reduction in levels of poly(GP) dipeptide. Suppression of CSF levels of a C9ORF72 polydipeptide has not previously been reported in humans. There is substantial evidence that significant pathology is derived from the C9ORF72 polydipeptides[12,15,41–45], and directly toxic effects of the expanded RNA transcript have also been described[46]. Our findings strongly encourage the view that suppressing the expression of the mutant alleles of *C9ORF72* might be clinically beneficial, regardless of whether the primary benefit is mediated by reduction in mutant transcripts or polydipeptide levels. Larger clinical trials now underway to assess the clinical effect of therapies that silence *C9ORF72* will likely illuminate this hypothesis.

Online content

Any methods, additional references, Nature Research reporting summaries, source data, extended data, supplementary information, acknowledgements, peer review information; details of author contributions and competing interests; and statements of data and code availability are available at https://doi.org/10.1038/s41591-021-01557-6.

Received: 5 February 2021; Accepted: 27 September 2021;
Published online: 23 December 2021

References

1. Dejesus-Hernandez, M. et al. Expanded GGGGCC hexanucleotide repeat in noncoding region of *C9ORF72* causes chromosome 9p-linked FTD and ALS. *Neuron* **72**, 245–256 (2011).
2. Renton, A. E. et al. A hexanucleotide repeat expansion in *C9ORF72* is the cause of chromosome 9p21-linked ALS-FTD. *Neuron* **72**, 257–268 (2011).
3. Cook, C. & Petrucelli, L. Genetic convergence brings clarity to the enigmatic red line in ALS. *Neuron* **101**, 1057–1069 (2019).
4. Amick, J. & Ferguson, S. M. C9orf72: at the intersection of lysosome cell biology and neurodegenerative disease. *Traffic* **18**, 267–276 (2017).
5. Belzil, V. V. et al. Reduced *C9orf72* gene expression in c9FTD/ALS is caused by histone trimethylation, an epigenetic event detectable in blood. *Acta Neuropathol.* **126**, 895–905 (2013).
6. Zhu, Q. et al. Reduced C9ORF72 function exacerbates gain of toxicity from ALS/FTD-causing repeat expansion in *C9orf72*. *Nat. Neurosci.* **23**, 615–624 (2020).
7. O'Rourke, J. G. et al. *C9orf72* is required for proper macrophage and microglial function in mice. *Science* **351**, 1324–1329 (2016).
8. Burberry, A. et al. Loss-of-function mutations in the *C9ORF72* mouse ortholog cause fatal autoimmune disease. *Sci. Transl. Med.* **8**, 347ra393 (2016).
9. Shi, Y. et al. Haploinsufficiency leads to neurodegeneration in *C9ORF72* ALS/FTD human induced motor neurons. *Nat. Med.* **24**, 313–325 (2018).
10. Ash, P. E. et al. Unconventional translation of *C9ORF72* GGGGCC expansion generates insoluble polypeptides specific to c9FTD/ALS. *Neuron* **77**, 639–646 (2013).
11. Mori, K. et al. The *C9orf72* GGGGCC repeat is translated into aggregating dipeptide-repeat proteins in FTLD/ALS. *Science* **339**, 1335–1338 (2013).
12. Mizielinska, S. et al. *C9orf72* repeat expansions cause neurodegeneration in *Drosophila* through arginine-rich proteins. *Science* **345**, 1192–1194 (2014).
13. Tao, Z. et al. Nucleolar stress and impaired stress granule formation contribute to *C9orf72* RAN translation-induced cytotoxicity. *Hum. Mol. Genet.* **24**, 2426–2441 (2015).
14. Freibaum, B. D. et al. GGGGCC repeat expansion in *C9orf72* compromises nucleocytoplasmic transport. *Nature* **525**, 129–133 (2015).
15. Loveland, A.B. et al. Ribosome inhibition by *C9orf72*-ALS/FTD poly-PR and poly-GR proteins revealed by cryo-EM. Preprint at https://www.biorxiv.org/content/10.1101/2020.08.30.274597v1 (2020).
16. Khvorova, A. & Watts, J. K. The chemical evolution of oligonucleotide therapies of clinical utility. *Nat. Biotechnol.* **35**, 238–248 (2017).
17. Jafar-Nejad, P. et al. The atlas of RNase H antisense oligonucleotide distribution and activity in the CNS of rodents and non-human primates following central administration. *Nucleic Acids Res.* **49**, 657–673 (2020).
18. Peters, O. M. et al. Human *C9ORF72* hexanucleotide expansion reproduces RNA foci and dipeptide repeat proteins but not neurodegeneration in BAC transgenic mice. *Neuron* **88**, 902–909 (2015).
19. O'Rourke, J. G. et al. *C9orf72* BAC transgenic mice display typical pathologic features of ALS/FTD. *Neuron* **88**, 892–901 (2015).
20. Donnelly, C. J. et al. RNA toxicity from the ALS/FTD *C9ORF72* expansion is mitigated by antisense intervention. *Neuron* **80**, 415–428 (2013).
21. Sareen, D. et al. Targeting RNA foci in iPSC-derived motor neurons from ALS patients with a *C9ORF72* repeat expansion. *Sci. Transl. Med.* **5**, 208ra149 (2013).
22. Lagier-Tourenne, C. et al. Targeted degradation of sense and antisense *C9orf72* RNA foci as therapy for ALS and frontotemporal degeneration. *Proc. Natl Acad. Sci. USA* **110**, E4530–E4539 (2013).
23. Jiang, J. et al. Gain of toxicity from ALS/FTD-linked repeat expansions in *C9ORF72* is alleviated by antisense oligonucleotides targeting GGGGCC-containing RNAs. *Neuron* **90**, 535–550 (2016).
24. Gendron, T. F. et al. Poly(GP) proteins are a useful pharmacodynamic marker for *C9ORF72*-associated amyotrophic lateral sclerosis. *Sci. Transl. Med.* **9**, eaai7866 (2017).
25. Cook, C. N. et al. *C9orf72* poly(GR) aggregation induces TDP-43 proteinopathy. *Sci. Transl. Med.* **12**, eabb3774 (2020).
26. Zhang, K. et al. The *C9orf72* repeat expansion disrupts nucleocytoplasmic transport. *Nature* **525**, 56–61 (2015).
27. Almeida, S. et al. Modeling key pathological features of frontotemporal dementia with *C9ORF72* repeat expansion in iPSC-derived human neurons. *Acta Neuropathol.* **126**, 385–399 (2013).
28. Zu, T. et al. RAN proteins and RNA foci from antisense transcripts in *C9ORF72* ALS and frontotemporal dementia. *Proc. Natl Acad. Sci. USA* **110**, E4968–E4977 (2013).
29. Rigo, F. et al. Pharmacology of a central nervous system delivered 2′-O-methoxyethyl-modified survival of motor neuron splicing oligonucleotide in mice and nonhuman primates. *J. Pharmacol. Exp. Ther.* **350**, 46–55 (2014).
30. Eckstein, F. Phosphorothioates, essential components of therapeutic oligonucleotides. *Nucleic Acid Ther.* **24**, 374–387 (2014).
31. Sztainberg, Y. et al. Reversal of phenotypes in *MECP2* duplication mice using genetic rescue or antisense oligonucleotides. *Nature* **528**, 123–126 (2015).
32. Becker, L. A. et al. Therapeutic reduction of ataxin-2 extends lifespan and reduces pathology in TDP-43 mice. *Nature* **544**, 367–371 (2017).
33. Tabrizi, S. J. et al. Targeting Huntingtin expression in patients with Huntington's disease. *N. Engl. J. Med.* **380**, 2307–2316 (2019).
34. Moazami, M.P. et al. Quantifying and mitigating motor phenotypes induced by antisense oligonucleotides in the central nervous system. Preprint at https://www.biorxiv.org/content/10.1101/2021.02.14.431096v1 (2021).

35. Waite, A. J. et al. Reduced C9orf72 protein levels in frontal cortex of amyotrophic lateral sclerosis and frontotemporal degeneration brain with the *C9ORF72* hexanucleotide repeat expansion. *Neurobiol. Aging* **35**, 1779. e5–1779.e13 (2014).
36. Meng, L. et al. Towards a therapy for Angelman syndrome by targeting a long non-coding RNA. *Nature* **518**, 409–412 (2015).
37. Zhao, H. T. et al. LRRK2 antisense oligonucleotides ameliorate α-synuclein inclusion formation in a Parkinson's disease mouse model. *Mol. Ther. Nucleic Acids* **8**, 508–519 (2017).
38. Mohan, A. et al. Antisense oligonucleotides selectively suppress target RNA in nociceptive neurons of the pain system and can ameliorate mechanical pain. *Pain* **159**, 139–149 (2018).
39. McCampbell, A. et al. Antisense oligonucleotides extend survival and reverse decrement in muscle response in ALS models. *J. Clin. Invest.* **128**, 3558–3567 (2018).
40. Tabrizi, S. J., Smith, A. V. & Bennett, C. F. Targeting Huntingtin in patients with Huntington's disease. Reply. *N. Engl. J. Med.* **381**, 1181–1182 (2019).
41. Aditi, Aditi, Folkmann, A. W. & Wente, S. R. Cytoplasmic hGle1A regulates stress granules by modulation of translation. *Mol. Biol. Cell* **26**, 1476–1490 (2015).
42. Jovicic, A. et al. Modifiers of *C9orf72* dipeptide repeat toxicity connect nucleocytoplasmic transport defects to FTD/ALS. *Nat. Neurosci.* **18**, 1226–1229 (2015).
43. Zhang, Y. J. et al. Poly(GR) impairs protein translation and stress granule dynamics in *C9orf72*-associated frontotemporal dementia and amyotrophic lateral sclerosis. *Nat. Med.* **24**, 1136–1142 (2018).
44. Yuva-Aydemir, Y., Almeida, S., Krishnan, G., Gendron, T. F. & Gao, F. B. Transcription elongation factor AFF2/FMR2 regulates expression of expanded GGGGCC repeat-containing *C9ORF72* allele in ALS/FTD. *Nat. Commun.* **10**, 5466 (2019).
45. Moens, T. G. et al. *C9orf72* arginine-rich dipeptide proteins interact with ribosomal proteins in vivo to induce a toxic translational arrest that is rescued by eIF1A. *Acta Neuropathol.* **137**, 487–500 (2019).
46. Coyne, A.N. et al. G_4C_2 repeat RNA initiates a POM121-mediated reduction in specific nucleoporins in C9orf72 ALS/FTD. *Neuron* **107**, 1124–1140 (2020).

Methods

Design of mouse and human studies. The goal of this study was to develop an ASO as a potential clinical therapeutic candidate to treat C9-ALS/FTD. Our experimental approach combined C9 patient-derived samples to evaluate selective efficacy in vitro and C9BAC transgenic mice to assess safety, efficacy and duration of effect in vivo. Per experiment, all mice were age-matched and randomly assigned to control or experimental group. Samples and data were collected in a blinded manner, processed and quantified. Molecular and physiological readouts include expression level of V1–V3 repeat-containing transcripts, all transcripts and peptides, weight of body and organs and motor functions. All outliers were included in data analysis. Exploratory experiments were performed on at least five mice per genotype. Sample size was calculated using the G-power analysis method based on previously defined effect size and standard deviation measuring variability within the sample.

The flow chart for the clinical study is presented in Fig. 3. This study was conducted with approval from the University of Massachusetts Medical School and the Western Institutional Review Board (no. 20183136) as well as the FDA (IND141673). Our initial spinal fluid evaluation was performed under the auspices of a longitudinal biomarker study (University of Massachusetts Medical School IRB docket no. 14341). Patient consent was obtained for these investigations as approved by the IRB.

ASOs. LNA phosphoramidites were synthesized in-house using standard methods[47] from the 3′-hydroxyl precursors. All other phosphoramidites were purchased from ChemGenes. 0.1 M DDTT (ChemGenes) was used as the sulfurizing reagent, and 0.25 M BTT (AIC) was used as the activator. ASOs were synthesized on a Dr. Oligo 48, ABI 394, AKTA Oligopilot 10 or AKTA Oligopilot 100 synthesizer, according to the required scale. LNA and MOE phosphoramidites were coupled for 8 min. Oligonucleotides were de-protected in concentrated aqueous ammonia at 55 °C for 18 h and purified using ion exchange chromatography (eluting with 30% acetonitrile in water containing increasing gradients of $NaClO_4$). Final purification, de-salting, concentration and pH adjustment were effected by diafiltration in an Amicon centrifugal filter. All oligonucleotides were characterized by liquid chromatography–mass spectrometry.

Dual-Luciferase Reporter Assay System. C9 intron 1 containing two G_4C_2 motifs (334 nucleotides 5′ of the G_4C_2 repeat motif and 769 nucleotides in the 3′ end) was amplified from blood genomic DNA using the following forward and reverse primers, 5′-acgtatgcggccgcacgtaacctacggtgtc-3′ and 5′-atacgtgcggccgctaccatcagtcaagtgatg-3′, and was cloned into the psiCHECK-2 vector (Promega). C9 intron 1 expression was measured with the Dual-Luciferase Reporter Assay System (Promega) according to the manufacturer's instructions.

Cell culture. *HEK293T cells.* HEK293T cells were transfected with 6.5 µg of psiCHECK-2 vector containing C9 intron 1 using Lipofectamine 3000 with P3000 reagent according to the manufacturer instructions (Thermo Fisher Scientific) in T25 flasks. One day after transfection, cells were plated into a 96-well plate in DMEM supplemented with 10% FBS and treated with the indicated dose of ASO the next day using Lipofectamine RNAiMax Reagent (Thermo Fisher Scientific). Cells were lysed for 48 h after ASO treatment, and luciferase signals were quantified.

C9 patient-derived fibroblasts. Skin biopsies obtained from two unrelated C9 carriers were cut into small pieces and placed on a culture dish with DMEM supplemented with 15% FBS to allow fibroblasts to expand. ASO treatment was performed on cells plated in a 10-cm dish using Lipofectamine RNAiMax Reagent. Total RNA was isolated 72 h after treatment.

C9BAC-derived primary cortical neurons. Embryos were removed at embryonic day 15.5 from pregnant WT C57BL/6 females crossed with homozygous C9BAC males. Cortical tissue of each embryo was dissected on ice-cold Hank's Balanced Salt Solution (Thermo Fisher Scientific). Pooled tissue was minced and digested with 0.05% Trypsin-EDTA (Life Technologies) at 37 °C for 12 min. Digestion was halted by the addition of 10% FBS/DMEM. Cells were triturated, resuspended in neurobasal media supplemented with GlutaMAX (Thermo Fisher Scientific), 2% penicillin–streptomycin and B27 supplement (Thermo Fisher Scientific) and seeded at 0.5×10^6 cells per well in six-well plates pre-coated with poly-L-ornithine (Sigma). Neurons were treated with ASO at the indicated dose 5 d after culture and collected 15 d after treatment.

***C9ORF72* BAC transgenic mice.** C9BAC mice were generated as previously described[18] and back-crossed to C57BL/6. All experimental protocols and procedures were approved by the University of Massachusetts Medical School Institutional Animal Care and Use Committee.

Stereotaxic pump implantation and bolus injection of ASO in the mouse brain. For ICV infusion of ASO or PBS vehicle through a micro-osmotic pump (Alzet pump model 1007D attached to Alzet Brain Infusion Kit 3), WT C57BL/6 or C9BAC transgenic mice were anesthetized and maintained on 2.5% isoflurane via a nose cone under a stereotaxic frame. The implantation procedure was performed as previously described[48], with a 3-mm cannula implantation 0.2 mm posterior and 1.0 mm lateral to the right of bregma.

For ICV bolus injection, mice were anesthetized with isoflurane and placed into a stereotaxic frame. Ten microliters of sterile PBS or ASO was injected into the right lateral ventricle using the following coordinates: 0.2 mm posterior and 1.0 mm lateral to the right from bregma and lowered to a depth of 3 mm.

Mouse behavior monitoring. Over the course of treatment and immediately before sacrifice, each animal was weighed and evaluated weekly in a blinded manner by a trained observer for adverse events, defined as any behavior not typical in a naive matched control animal, including, but not limited to, limb clasping, tremors, abnormal respiration, paralysis, spasticity, impaired reflex, hyperactivity and lethargy.

Rotarod. Coordinated motor functions were assessed in control and treated mice using the rotarod test, as previously described[18]. In brief, mice were tested weekly beginning 2 weeks before ASO/vehicle administration and ending at the week of sacrifice. Each animal was given three trials on a 4–40-r.p.m. accelerating rotarod for 5 min with a 1-min intertrial interval. Latencies to fall for each animal were automatically recorded by a computer and plotted as mean ± s.e.m.

Blood biochemistry. Whole blood samples were collected after cardiac puncture (terminal procedure). Blood biochemistry was performed using the VetScan Comprehensive Diagnostic Profile (Abaxis).

Southern blot. Southern blot was performed on 10-µg genomic DNA isolated using a Gentra Puregene Tissue Kit (Qiagen). DNA was digested overnight with AluI and DdeI at 37 °C and separated by electrophoresis on a 0.6% agarose gel, transferred to a positively charged nylon membrane (Roche Applied Science), cross-linked by UV and hybridized overnight at 55 °C with a digoxigenin-labeled G_2C_4 DNA probe in hybridization mix buffer (Easy Hyb, Roche). The digoxigenin-labeled probe was detected with anti-digoxigenin antibody and CDP-Star reagent as recommended by the manufacturer (Roche).

RNA extraction and qRT–PCR. Total RNA was isolated from snap-frozen cortex or spinal cord tissue using TRIzol (Thermo Fisher Scientific) and subsequently treated with DNase I (Qiagen). Then, 1 µg of total RNA was reverse transcribed into cDNA using random hexamers and MultiScribe Reverse Transcriptase (Thermo Fisher Scientific) following the manufacturer's instructions. Quantitative PCR was performed on a StepOnePlus Real-Time PCR system using SYBR Green Master Mix (Applied Biosystems) and 0.2 µM of forward and reverse primers as described in ref. [41]. Cycle threshold (Ct) values for each sample and gene were normalized to *GAPDH*. The 2exp (−ΔΔCt) method was used to determine the relative expression of each target gene.

Fluorescence in situ hybridization. Fluorescence in situ hybridization was performed as previously described[49] using a 5′ end Cy3-conjugated $(G_2C_4)_4$ oligonucleotide DNA probe at 55 °C in hybridization buffer containing formamide 40%/2× SSC/0.1% Tween 20/DNA salmon sperm. Samples were then washed twice in pre-warmed wash buffer (formamide 40%/2× SSC/0.1% Tween 20) and in stringency wash buffer (0.2× SSC/0.1% Tween 20) at 55 °C. Samples were then mounted in ProLong Gold Antifade reagent with DAPI (Thermo Fisher Scientific). Confocal images were taken with a Leica TCS SP5 II laser scanning confocal microscope and processed with Leica LAS AF software.

Detection of poly(GP) and poly(PR). Rabbit polyclonal anti-poly(GP) and PR antibodies were generated to the repeat motif (GP_8, PR_8) by New England Peptide. Poly(GP) or poly(PR) levels in lysates were measured using a sandwich immunoassay that uses Meso Scale Discovery (MSD) electrochemiluminescence detection technology. Tissue samples were lysed in RIPA buffer supplemented with 1× Roche cOmplete Protease Inhibitor and 1× Halt Phosphatase Inhibitor Cocktail (Thermo Fisher Scientific) using TissueLyserII (Qiagen) followed by sonication on ice. Samples were gently homogenized on a rocker at 4 °C for 30 min. Debris was removed by centrifugation (15 min, 14,000*g*, 4 °C), and the supernatant was collected. Total protein concentration was determined using the BCA Protein Assay Kit (Thermo Fisher Scientific). Next, 50 µg of total protein diluted in PBS-Tween supplemented with 10% FBS was loaded per well in duplicate wells. Serial dilutions of recombinant $(GP)_8$ or $(PR)_8$ spiked in WT C57Bl/6 brain protein extracts were used to prepare the standard curve. Response values corresponding to the intensity of emitted light upon electrochemical stimulation of the assay plate using the MSD QuickPlex SQ120 were acquired and background-corrected using the average response from lysates obtained from WT C57Bl/6 brain extract.

Detection of phosphorylated neurofilament heavy chain and neurofilament light chain. Neurofilament light chain (NFL) and phosphorylated neurofilament heavy chain (pNFH) were detected in CSF samples using sandwich immunoassays and the MSD QuickPlex SQ120. For pNFH measures, the Iron Horse Diagnostics clinically validated assay was used with a monoclonal anti-pNFH antibody as

capture and sulfo-tagged polyclonal anti-pNFH antibody for detection. Purified pNFH was used to generate a calibration curve. All assays were performed in triplicate with a coefficient of variation (CV) of less than 5% for all samples. The lower limit of quantification of the pNFH assay is 1.2 pg ml^{-1} in CSF. For NFL measures, a R-PLEX human NFL MSD assay kit was used (MSD cat. no. F217X) following manufacturer specifications. All assays were performed in triplicate with a CV of less than 5% for all samples. The lower limit of quantification of the NFL assay is 2.0 pg ml^{-1}.

Immunohistochemistry. Brains were rapidly removed from euthanized animals. The contralateral hemibrain was post-fixed in 10% formalin. Paraffin-embedded or cryoprotected blocks were cut in 10-µm-thick sagittal sections. Slides were permeabilized with Triton 0.1% for 10 min. Non-specific antibody binding was blocked by incubation with 10% goat serum in PBS-Tween 0.01% for 1 h. Primary antibodies were diluted in blocking solution, and sections were incubated overnight at 4 °C. After three washes in PBS-Tween 0.01%, sections were incubated with Alexa Fluor 488 or Alexa Fluor 546 conjugated secondary antibodies diluted in PBS for 1 h at room temperature. Autofluorescence was quenched by slide immersion in 0.5% Sudan Black B in 70% ethanol, and cell nuclei were stained with DAPI. Primary antibodies used included mouse anti-NeuN (1:500, Millipore) and rabbit anti-P/S ASO (1:500, in-house). In brief, a rabbit polyclonal antibody was raised in-house by inoculating two female New Zealand White rabbits with a fully PS-modified, KLH-conjugated ASO. Boosts and bleeds were carried out at regular intervals over 1 year, and antisera were used for histology (Moazami and Watts, in preparation).

H&E staining. Next, 8–10-µm-thick sections of mouse liver and kidney were cut from formalin-fixed, paraffin-embedded blocks. Standard H&E staining was performed.

Mass spectrometric characterization of clinical ASO. The sequence and modification pattern of ASO5-2 was confirmed by mass spectrometric (MS) analysis performed by nanoflow electrospray ionization (that is, nanospray) on a Fourier transform ion cyclotron resonance (FTICR) mass spectrometer (vide infra for conditions). The multiply charged ions observed in negative ion mode (Supplementary Fig. 4a) provided a monoisotopic molecular mass of 6,461.1894 u, which matched very closely the expected value of 6,461.1888 Da calculated from sequence. In subsequent experiments, the $[M - 4H]^{4-}$ molecular ion at 1,615 *m/z* was submitted to tandem mass spectrometry (MS^2) to achieve sequence confirmation (vide infra). Upon isolation in the mass selective quadrupole (Q) and activation by collisions with Ar in the collision cell (q), the precursor ion exhibited typical fragment series corresponding to the central region of the construct, which confirmed the sequence spanning from A7 to C13 (Supplementary Fig. 5b). Distinctive signals were additionally detected at 1,179 and 1,971 *m/z*, which were assigned to fragments corresponding to the entire G1:T6 and G14:C18 moieties, respectively. In turn, each of these first-generation fragments was individually isolated and activated in the FTICR cell to complete MS^3 determinations (Supplementary Fig. 5c,d). These experiments provided abundant second-generation fragments that confirmed the sequences of the construct's terminal regions.

All analyses were carried out on a Bruker 12T solariX FTICR equipped with a 12T superconducting magnet and a home-built ion source that enabled static nanospray operations. No sample de-salting or chromatographic steps were employed. All samples consisted of a 4 µM solution of ASO5-2 in 150 mM ammonium acetate (pH 7.4) and 10% volume of 2-propanol. In each analysis, a 5-ml aliquot was loaded onto a quartz emitter prepared in-house. A stainless steel wire was inserted from the back end to provide the voltage necessary to achieve a stable spray. The instrument was calibrated by using a 1 mg ml^{-1} CsI solution that provided an accuracy of 87 p.p.b. Detection was accomplished in broadband mode, which afforded a typical 230,000 resolution. The first activation step was carried out in the collision cell (q) of the instrument, which was flooded with a low pressure of Ar and subjected to an 18.5-V activation voltage. The second activation step was carried out in the FTICR cell by irradiating selected ions with a frequency that was 250 Hz off-resonance and 0.65–1.29% power. The data were processed by using the DataAnalysis package provided by Bruker. The results were interpreted by using the Mongo Oligo Mass Calculator, version 2.08, available at https://mods.rna.albany.edu/masspec/Mongo-Oligo.

Oligonucleotide pharmacokinetics. Patient CSF was stored at −80 °C until analysis. ASO levels in patient CSF were quantified using an assay based on splint ligation and qPCR as previously described[50]. CSF from the same patient before treatment was added to the hybridization mixture and spiked with a known concentration series of ASO to generate a standard curve. Sequences of oligonucleotides used for detection of ASO5-2 were as follows: Probe A: 5′-CTCGACCTCTCTATGGGCAGTCACGACAGGAGTCGCGCG-3′ ; Probe B: 5′-pCTAGGGGCCGCTGAGTCGGAGACACGCAGGGCTTAA -3′; Forward primer: 5′-GCTCGACCTCTCTATGGGC-3′; Reverse primer: 5′-TTAAGCCCTGCGTGTCTCC-3′; and Double-quenched probe: 5′/FAM/CTAGCGCGC/ZEN/GACTCCGTCGTG/IABkFQ/-3′.

Fitting ASO levels to a two-stage exponential clearance model allowed an excellent fit with empirically measured ASO levels (Supplementary Fig. 6).

Statistical analysis. All data were graphed as mean ± s.e.m., showing data points, and statistics were analyzed using GraphPad Prism software (version 9.1.1). Tests between multiple groups (comparisons indicated in the corresponding figure legends) used one-way ANOVA corrected with Dunnett's multiple comparisons post hoc test: $^*P < 0.05$, $^{**}P < 0.01$, $^{***}P < 0.001$ and $^{****}P < 0.0001$; NS, not significant.

Reporting Summary. Further information on research design is available in the Nature Research Reporting Summary linked to this article.

Data availability

The data supporting the findings of this study are available within the main text and the Supplementary Information. The full clinical trial protocol for this study is available upon reasonable request to the corresponding authors. C9BAC mice and PS-targeted polyclonal antibody are available by contacting the investigators.

References

47. Kumar, R. et al. The first analogues of LNA (locked nucleic acids): phosphorothioate-LNA and 2′-thio-LNA. *Bioorg. Med. Chem. Lett.* **8**, 2219–2222 (1998).
48. DeVos, S.L. & Miller, T.M. Direct intraventricular delivery of drugs to the rodent central nervous system. *J. Vis. Exp.* e50326 (2013).
49. Tran, H. et al. Differential toxicity of nuclear RNA foci versus dipeptide repeat proteins in a *Drosophila* model of *C9ORF72* FTD/ALS. *Neuron* **87**, 1207–1214 (2015).
50. Shin, M., Krishnamurthy, P. M., Devi, G. & Watts, J. K. Quantification of antisense oligonucleotides by splint ligation and quantitative polymerase chain reaction. Nucleic Acid Ther. https://doi.org/10.1089/nat.2021.0040 (in the press) (2021).

Acknowledgements

The authors thank the Brown and Watts laboratories, Wave Life Sciences, the Animal Medicine and DERC Morphology Cores and F. Ladam for advice, technical support and manuscript review. Funding: This work was funded by the National Institutes of Health (R01 NS111990 to R.H.B. and J.K.W.), the Angel Fund for ALS Research and the Ono Pharmaceutical Foundation (Breakthrough Science Award to J.K.W.). R.H.B. also acknowledges funding from ALSOne, ALS Finding a Cure, the Cellucci Fund for ALS Research and the Max Rosenfeld Fund. We also acknowledge the NEALS Biorepository for providing all or part of the biofluids from the ALS, healthy controls and non-ALS neurological controls used in this study. The project described in this publication was supported, in part, by the University of Massachusetts Clinical and Translational Science Award (no. UL1TR001453) from the National Center for Advancing Translational Sciences of the National Institutes of Health. The content is solely the responsibility of the authors and does not necessarily represent the official views of the National Institutes of Health.

Author contributions

R.H.B. conceived the project. H.T., R.H.B., J.K.W. and M.P.M. designed the experimental plan. M.P.M. performed oligo synthesis. M.P.M., C.P., J.M. and A.W. supported the mouse experiments. H.T., H.Y. and N.W. processed the cell and mouse tissue experiments. M.P.M. raised the PS-targeted antibody and performed brain staining. T.K. and D.F. verified the sequence of the clinical ASO. N.S. and C.D. prepared the drug product for clinical use. R.H.B., D.M.-Y. and C.L.D. supported the clinical work, including preparing consent forms. H.G.-E., M.P.M., M.M. and R.M.K. supported the sheep studies. M.S. and N.W. evaluated ASO levels in patient CSF. H.T., R.H.B. and J.K.W. wrote manuscript. R.H.B. and J.K.W. supervised the project.

Competing interests

The authors have filed a patent related to this research. R.H.B. is a co-founder of Apic Bio.

Additional information

Supplementary information The online version contains supplementary material available at https://doi.org/10.1038/s41591-021-01557-6.

Correspondence and requests for materials should be addressed to Jonathan K. Watts or Robert H. Brown.

Peer review information *Nature Medicine* thanks Aaron Gitler and the other, anonymous, reviewer(s) for their contribution to the peer review of this work. Jerome Staal was the primary editor on this article and managed its editorial process and peer review in collaboration with the rest of the editorial team.

nature research

Corresponding author(s): Robert H. Brown, Jr., D.Phil., M.D.
Jonathan Watts, Ph.D.

Last updated by author(s): 2021-July-22

Reporting Summary

Nature Research wishes to improve the reproducibility of the work that we publish. This form provides structure for consistency and transparency in reporting. For further information on Nature Research policies, see our Editorial Policies and the Editorial Policy Checklist.

Statistics

For all statistical analyses, confirm that the following items are present in the figure legend, table legend, main text, or Methods section.

n/a	Confirmed	
☐	☒	The exact sample size (*n*) for each experimental group/condition, given as a discrete number and unit of measurement
☐	☒	A statement on whether measurements were taken from distinct samples or whether the same sample was measured repeatedly
☐	☒	The statistical test(s) used AND whether they are one- or two-sided *Only common tests should be described solely by name; describe more complex techniques in the Methods section.*
☒	☐	A description of all covariates tested
☒	☐	A description of any assumptions or corrections, such as tests of normality and adjustment for multiple comparisons
☐	☒	A full description of the statistical parameters including central tendency (e.g. means) or other basic estimates (e.g. regression coefficient) AND variation (e.g. standard deviation) or associated estimates of uncertainty (e.g. confidence intervals)
☐	☒	For null hypothesis testing, the test statistic (e.g. *F*, *t*, *r*) with confidence intervals, effect sizes, degrees of freedom and *P* value noted *Give P values as exact values whenever suitable.*
☒	☐	For Bayesian analysis, information on the choice of priors and Markov chain Monte Carlo settings
☒	☐	For hierarchical and complex designs, identification of the appropriate level for tests and full reporting of outcomes
☒	☐	Estimates of effect sizes (e.g. Cohen's *d*, Pearson's *r*), indicating how they were calculated

Our web collection on statistics for biologists contains articles on many of the points above.

Software and code

Policy information about availability of computer code

Data collection	Leica LAS AF was used to collect microscopic images.
Data analysis	GraphPad Prism 9.1.1 was used for visualization and statistical analysis.

For manuscripts utilizing custom algorithms or software that are central to the research but not yet described in published literature, software must be made available to editors and reviewers. We strongly encourage code deposition in a community repository (e.g. GitHub). See the Nature Research guidelines for submitting code & software for further information.

Data

Policy information about availability of data

All manuscripts must include a data availability statement. This statement should provide the following information, where applicable:

- Accession codes, unique identifiers, or web links for publicly available datasets
- A list of figures that have associated raw data
- A description of any restrictions on data availability

Critical data are summarized in Figures 1, 2 and 3. The data supporting the findings of this study are available within the main text and the supplementary information. The full clinical trial protocol for this study is available upon request to the corresponding authors.

Field-specific reporting

Please select the one below that is the best fit for your research. If you are not sure, read the appropriate sections before making your selection.

☒ Life sciences ☐ Behavioural & social sciences ☐ Ecological, evolutionary & environmental sciences

For a reference copy of the document with all sections, see nature.com/documents/nr-reporting-summary-flat.pdf

Life sciences study design

All studies must disclose on these points even when the disclosure is negative.

Sample size	In this pilot study, data are reported from one individual. Mouse experiments included groups of 5-7 mice.
Data exclusions	None
Replication	The critical outcome findings in the patient's CSF were replicated multiple times. For mouse studies, the experiments were repeated multiple times by multiple investigators and with sufficiently large sample sizes (5-7 mice per group). Cell studies included at least three independent biological replicates (experiments carried out on separate days). All replication experiments with both mice and cells were successful.
Randomization	Mice were randomly allocated into different groups. For cell experiments, cell plates were randomly allocated to the different experimental groups.
Blinding	For cell experiments, investigators were blinded to group allocation during data collection and analysis. During the mouse experiments and poly(GP) analysis, investigators were again blinded to sample identity and group allocation during data collection and analysis.

Reporting for specific materials, systems and methods

We require information from authors about some types of materials, experimental systems and methods used in many studies. Here, indicate whether each material, system or method listed is relevant to your study. If you are not sure if a list item applies to your research, read the appropriate section before selecting a response.

Materials & experimental systems

n/a	Involved in the study
☐	☒ Antibodies
☐	☒ Eukaryotic cell lines
☒	☐ Palaeontology and archaeology
☐	☒ Animals and other organisms
☐	☒ Human research participants
☐	☒ Clinical data
☒	☐ Dual use research of concern

Methods

n/a	Involved in the study
☒	☐ ChIP-seq
☒	☐ Flow cytometry
☒	☐ MRI-based neuroimaging

Antibodies

Antibodies used	1 .anti-NeuN (Millipore, cat no. MAB377, dilution 1/500)) 2. anti-PS-ASO (polyclonal rabbit antibody raised at UMass Medical School, Watts Lab, diluation 1/500) 3. anti-phosphorylated NFH (assay run at Iron Horse Diagnostics) 4. anti-NFL (assay run at Iron Horse Diagnostics) 5. anti-GP (polyclonal rabbit antibody, UMass Medical School and New England Peptides, final concentration for ELISA 150 ucg/ml) 6. Donkey anti-mouse IgG, AlexaFluor 546, Life Technologies, cat. no. A10036, dilution 1/1000) 7. Goat anti-rabbit IgG, AlexaFluor 488, Cell Signalling, cat. no. 4412, dilution 1/1000) 8. Sheep anti-digoxigenin-AP Fab fragments, Roche Life Science, cat. no. 11093-274-910, 150 U/ 200 uL)
Validation	1. abcam.com/neun-antibody-1b7-ab104224.html 2. validated using appropriate controls in the Watts laboratory (parallel staining of non-ASO-treated mouse tissues to show that staining is ASO-specific; characterization of pAb binding affinity and specificity using in vitro assays; a separate publication is in progress). 3,4. validated for commercial use at Iron Horse Diagnostics 5. anti-GP antibody was validated using WT mouse and transgenic C9orf72 mouse brain lysates, and patient-derived CSF samples. GP specificity was further confirmed using recombinant GP, PR and GA synthetic peptides.

Eukaryotic cell lines

Policy information about cell lines

Cell line source(s)	Patient-derived fibroblasts HEK293 cells; ATCC, CRL-1573
Authentication	These lines were not authenticated.
Mycoplasma contamination	These lines were not tested for mycoplasma.
Commonly misidentified lines (See ICLAC register)	We did not find HEK293 cells listed in the ICLAC register.

Animals and other organisms

Policy information about studies involving animals; ARRIVE guidelines recommended for reporting animal research

Laboratory animals	C57B/J mice, males and females, typically at 5-6 months of age. The animals were maintained in a facility that runs on a 12 hour light/dark cycle. The light comes on at 7 am and turns off at 7 pm. The temperature range is 68-79deg F and the humidity range is 30-70%.
Wild animals	No wild animals were used in this study.
Field-collected samples	No field-collected samples were used in this study.
Ethics oversight	The animal studies were approved by the UMass Medical School IACUC.

Note that full information on the approval of the study protocol must also be provided in the manuscript.

Human research participants

Policy information about studies involving human research participants

Population characteristics	This pilot study enlisted one male, age 60, with amyotrophic lateral sclerosis arising from a hexanucleotide expansion in intron 1 of the C9ORF72 gene
Recruitment	This patient was from a family with four members afflicted with C9ORF72 ALS or ALS-FTD. He was well known to our laboratory when he developed recurrent foot drop, the first manifestation of his motor neuron disease. Though we had worked with this individual at length (because of his family history), the efficacy analysis in our study was predicated solely on CSF levels of the poly(GP) dipeptide, a parameter that in our view was objective and not subject to bias.
Ethics oversight	The protocol was approved by the Western Institutional Review board and also the FDA.

Note that full information on the approval of the study protocol must also be provided in the manuscript.

Clinical data

Policy information about clinical studies

All manuscripts should comply with the ICMJE guidelines for publication of clinical research and a completed CONSORT checklist must be included with all submissions.

Clinical trial registration	FDA file 141673, Western IRB 20183136
Study protocol	The protocol is available via request to the corresponding authors.
Data collection	Data were collected in (1) the clinical trials unit and neurology service at UMass Medical School and UMass Memorial Medical Center, which is run under the auspices of the Office of Clinical Research (https://www.umassmed.edu/ocr/clinical-research-center/), and (2) UMass Memorial Medical Center. The period in which we considered candidates for this pilot study began at the time of the original submission of our IND (October 18, 2018) and was completed shortly after the IND was approved (August 9, 2019). The period of collection of the data in this study began after informed consent was obtained and the first treatment was initiated (August 26, 2019) and continued through October 20, 2020. The study data also includes a single data point from an earlier study (May 19, 2016), that was also obtained with IRB approval and informed consent.
Outcomes	The primary outcome was safety; the secondary outcome was suppression of the C9ORF72 gene as determined by levels in the CSF of the GP polydipeptide. Safety was assessed using physical examination, blood study, electrocardiogram and cerebrospinal fluid parameters. The blood studies included complete blood count and metabolic profile (electrolytes, liver and renal function tests). CSF parameters included total and differential cell count, glucose and total protein, and levels of phosphorylated neurofilament heavy chain and neurofilament light chain.